

Research Article

Open Access



# Thermoelectric and mechanical performances of ionic liquid-modulated PEDOT:PSS/SWCNT composites at high temperatures

Wenjiang Deng<sup>1</sup>, Liang Deng<sup>1</sup>, Yue Hu<sup>1</sup>, Yichuan Zhang<sup>1,2</sup>, Guangming Chen<sup>1</sup>

<sup>1</sup>College of Materials Science and Engineering, Shenzhen University, Shenzhen 518055, Guangdong, China.

<sup>2</sup>State Key Laboratory of Polymer Materials Engineering, Sichuan University, Chengdu 610065, Sichuan, China.

**Correspondence to:** Prof. Yichuan Zhang, College of Materials Science and Engineering, Shenzhen University, Shenzhen 518055, Guangdong, China. E-mail: yichuan.zhang@szu.edu.cn; Prof. Guangming Chen, College of Materials Science and Engineering, Shenzhen University, Shenzhen 518055, Guangdong, China. E-mail: chengm@szu.edu.cn

**How to cite this article:** Deng W, Deng L, Hu Y, Zhang Y, Chen G. Thermoelectric and mechanical performances of ionic liquid-modulated PEDOT:PSS/SWCNT composites at high temperatures. *Soft Sci* 2021;1:14. <https://dx.doi.org/10.20517/ss.2021.17>

**Received:** 14 Oct 2021 **First Decision:** 2 Nov 2021 **Revised:** 29 Nov 2021 **Accepted:** 3 Dec 2021 **Published:** 8 Dec 2021

**Academic Editor:** Zhifeng Ren **Copy Editor:** Xi-Jun Chen **Production Editor:** Xi-Jun Chen

## Abstract

Significant progress has been achieved for flexible polymer thermoelectric (TE) composites in the last decade due to their potential application in wearable devices and sensors. In sharp contrast to the exceptional increase in TE studies at room temperature, the mechanical performance of polymer TE composites has received relatively less attention despite the significance of the application of TE composites in high-temperature environments. The TE and mechanical performances of flexible poly(3,4-ethylenedioxythiophene):poly(styrene sulfonate)/single-walled carbon nanotube (PEDOT:PSS/SWCNT) composite films with an ionic liquid (IL) (referred to as "PEDOT:PSS/SWCNT-IL") at high temperatures are studied in the present work. The fabricated composite films show increasing TE performance with increasing temperature and SWCNT content. The maximum value of the power factor reaches  $301.35 \mu\text{W m}^{-1} \text{K}^{-2}$  at 470 K for the PEDOT:PSS/SWCNT-IL composite. Furthermore, the addition of the IL improves the elongation at break of the composites compared to the IL-free composites. This work promotes the advancement of flexible polymer TE composites and widens their potential applications at different temperature ranges.

**Keywords:** Thermoelectrics, composite films, ionic liquids, mechanical performance



© The Author(s) 2021. **Open Access** This article is licensed under a Creative Commons Attribution 4.0 International License (<https://creativecommons.org/licenses/by/4.0/>), which permits unrestricted use, sharing, adaptation, distribution and reproduction in any medium or format, for any purpose, even commercially, as long as you give appropriate credit to the original author(s) and the source, provide a link to the Creative Commons license, and indicate if changes were made.



## INTRODUCTION

Thermoelectric (TE) materials have been studied extensively as a result of their unique ability to realize energy conversion between heat and electricity and their excellent potential for a range of versatile applications in complex environments to harvest waste heat<sup>[1-7]</sup>. TE conversion efficiency is reliant on TE performance, which is usually assessed by a dimensionless parameter known as the TE figure of merit ( $ZT = \sigma S^2 T / \kappa$ , where  $\sigma$ ,  $S$ ,  $\kappa$  and  $T$  are the electrical conductivity, Seebeck coefficient, thermal conductivity and absolute temperature, respectively). Furthermore, the power factor ( $PF = S^2 \sigma$ ) is also adopted to evaluate the TE performance of polymers and polymer composites due to their low or similar thermal conductivity<sup>[8]</sup>.

In recent decades, inorganic TE materials (e.g.,  $\text{Bi}_2\text{Te}_3$ ,  $\text{Sb}_2\text{Te}_3$  and their alloys) have been studied intensively due to their high TE performance<sup>[9-11]</sup>. However, their applications are impeded by their inevitable drawbacks that include intrinsic rigidity, toxicity, high cost and scarcity. Compared to their inorganic counterparts, conducting polymer (CP)-based flexible TE materials exhibit advantages such as intrinsic flexibility, low thermal conductivity and low toxicity. Poly(3,4-ethylenedioxythiophene) (PEDOT)<sup>[12,13]</sup>, polypyrrole<sup>[14,15]</sup> and polyaniline<sup>[16]</sup> are the main CPs for TE applications<sup>[17,18]</sup>. Of these, PEDOT is one of the most successful CPs as a result of its satisfactory TE performance and commercial availability. The main issue for improving the TE performance of CPs is their low electrical conductivity. CP/carbon nanotube (CNT) TE composites represent an effective alternative for improved TE performance by utilizing the effective interfacial  $\pi$ - $\pi$  conjugated interaction between CPs and CNTs<sup>[19,20]</sup>. Indeed, significant progress in the improvement of TE performance has been achieved for CP/CNT composites at room temperature<sup>[21-23]</sup>. However, their high-temperature TE performance has received significantly less attention than their room-temperature properties. In addition, it has been demonstrated that there is a trade-off between TE and mechanical performances<sup>[24-26]</sup>. The issue of whether this trade-off is valid or not has scarcely been discussed for CP/CNT composites at high temperatures. Although this trade-off is vital for the potential application of TE composites at high temperatures, the related properties of the composites remain unknown.

In our previous work, we reported the preparation of flexible PEDOT:poly(styrene sulfonate) (PSS)/single-walled (SW)CNT films with ionic liquid (IL) additives (referred to as "PEDOT:PSS/SWCNT-IL")<sup>[27]</sup>. The composite films showed an enhanced TE performance after the addition of IL into the system. In the present work, the temperature dependence of the TE performance of PEDOT:PSS/SWCNT-IL films is studied relative to IL-free PEDOT:PSS/SWCNT films. The carrier transport mechanism is discussed using the variable range hopping (VRH) model. The mechanical properties of PEDOT:PSS/SWCNT-IL and IL-free PEDOT:PSS/SWCNT are also evaluated at different high temperatures.

## EXPERIMENTAL

### Chemicals and materials

SWCNTs (purity of > 90 wt.% and diameter of 1-2 nm) were purchased from Shenzhen Nanotech Port Co., Ltd., China. A PEDOT:PSS aqueous dispersion with a solid content of 1.1 wt.% (Clevios PH 1000) was obtained from Heraeus Materials Technology Shanghai Ltd., China. The molecular formula of PEDOT:PSS is shown in Figure 1. 1-Butyl-3-(4-sulfobutyl)imidazolium trifluoromethanesulfonate IL 95% (HPLC grade) was provided by Shanghai Mackin Biochemical Co., Ltd., China and its molecular formula is shown in Figure 1. The selection of IL additives was based on their multiple roles in enhancing the TE performance of the PEDOT:PSS/SWCNT system<sup>[27]</sup>.

### Preparation of PEDOT/SWCNT films with IL

Figure 1 shows the preparation procedure of the flexible PEDOT/SWCNT films. Here, the fabrication procedure of a composite film of PEDOT:PSS/SWCNT (70/30 wt./wt.) with 50 wt.% IL is described as an

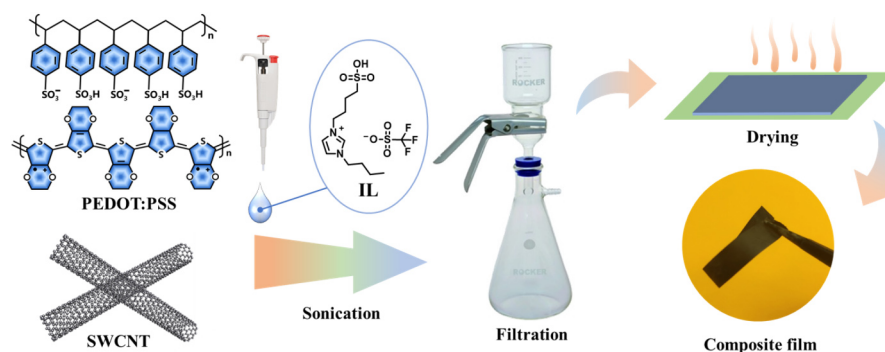


**Figure 1.** Schematic illustration of the preparation procedure for the PEDOT:PSS/SWCNT composite films with IL. PEDOT:PSS/SWCNT: Poly(3,4-ethylenedioxythiophene):poly(styrene sulfonate)/single-walled carbon nanotube; IL: ionic liquid.

example. In short, the SWCNTs (9.64 mg) and IL (8  $\mu$ L) were successively added to an ethanol solution and ultrasonically dispersed to form a homogeneous SWCNT dispersion containing the IL, followed by the addition of a PEDOT:PSS aqueous solution (2 mL) with 20 min of sonication to form a homogeneously dispersed PEDOT:PSS/SWCNT solution with the IL. The final composite film was obtained by vacuum filtration, repeated rinsing and vacuum drying [Figure 1]. The detailed preparation procedures can be found in our previous work<sup>[27]</sup>. For brevity, the PEDOT:PSS/SWCNT composites without IL and the PEDOT:PSS/SWCNT composites with an IL content of 50 wt.% are referred to as IL-free PEDOT:PSS/SWCNT and PEDOT:PSS/SWCNT-IL, respectively. The IL content was chosen at 50 wt.% because it is the optimal content for TE performance at room temperature<sup>[27]</sup>. As emphasized in our previous work<sup>[27]</sup>, the IL content is relative to the solid contents of PEDOT:PSS and SWCNTs, with the repeated rinsing procedure washing out most of the IL. Furthermore, for comparison, a pure SWCNT film (32.14 mg) and SWCNTs (32.14 mg) with an IL content of 50 wt.% were prepared without the addition of PEDOT:PSS.

### TE and mechanical performance measurements

The temperature dependencies of the electrical conductivities ( $\sigma$ ) and the Seebeck coefficients ( $S$ ) in a temperature range from 298 to 470 K were measured by a commercially available Thin-Film Change Temperature Thermoelectric Parameter Test System (MRS-3 CT, Wuhan Joule Yacht Science & Technology Co., Ltd., China), with a quasi-steady-state mode was applied. The TE performance was evaluated by the power factor ( $PF = \sigma S^2$ ) in the present work. The room-temperature tensile stress-strain measurements were performed using an EUT4103 testing instrument with a speed of 3 mm min<sup>-1</sup> at 298 and 470 K. The high-temperature tensile stress-strain measurements were performed with the same instrument with a temperature-controlled chamber at the target temperature.

### Structural and morphological characterization

The SWCNTs were observed with high-resolution scanning electronic microscopy (SEM, FEI APREO S). The statistical distribution of SWCNT bundles was analyzed using Image J software based on the SEM images. The carrier concentration and mobility were measured using an Ecopia HMS-3000 Hall effect measurement system. Thermogravimetric analysis (TGA) was performed on a TA TGA-Q50 thermal analysis system in a N<sub>2</sub> atmosphere from room temperature to 1073 K at a heating speed of 10 K min<sup>-1</sup>.

## RESULTS AND DISCUSSION

### Morphologies of neat SWCNT and SWCNT-IL films

Typical SEM images of the SWCNT and SWCNT-IL films are compared in Figure 2. Basically, SWCNTs in

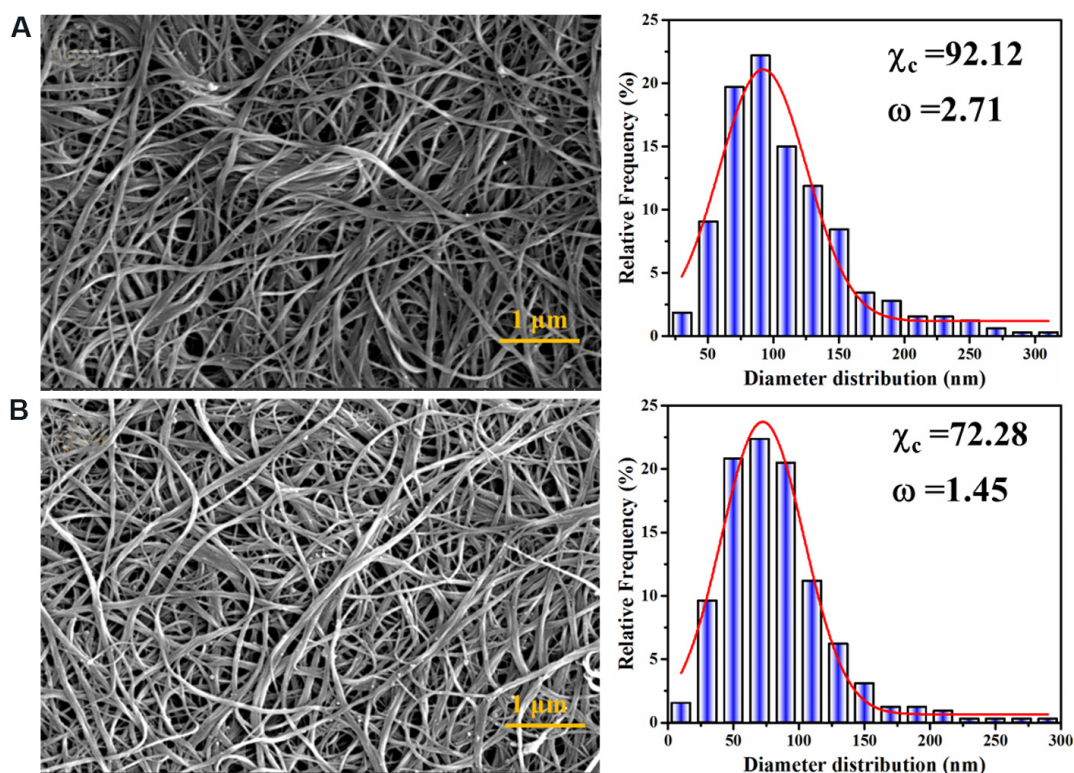


**Figure 2.** Scanning electronic microscopy images of (A) pure SWCNTs and (B) SWCNT-IL. Statistical distributions of the SWCNT bundle diameters are presented on the right. SWCNTs: Single-walled carbon nanotubes; IL: ionic liquid.

the form of bundles were observed in both samples. The diameters of the SWCNT bundles were measured at more than 300 diverse sites and the corresponding statistical histograms are shown at the right side of each SEM image. The mean values ( $\chi_c$ ) and standard deviations ( $\omega$ ) of the SWCNT bundles are used to characterize the diameter distributions in the histograms, which are fitted by a Gaussian distribution<sup>[28]</sup>:

$$y = y_0 + Ae^{-(x-\chi_c)^2/2\omega^2} \quad (1)$$

where  $x$  is the SWCNT bundle diameter (nm) and the parameters  $y$ ,  $y_0$ ,  $\chi_c$ ,  $\omega$  and  $A$  represent the count, offset, center position of the distribution fitting peak, width of the distribution and amplitude of the distribution, respectively. Apparently, the SWCNT film without IL has a higher  $\chi_c$  and there are more SWCNT bundles with larger diameters [Figure 2A]. After the IL is added,  $\chi_c$  decreases [Figure 2B], suggesting that the SWCNT dispersion is enhanced with the IL<sup>[27]</sup>.

### TE performance of composites with IL at high temperature

Figure 3 shows the TGA curve of the PEDOT:PSS-IL film, which indicates that the film can maintain its thermal stability up to 548 K. There is some mass loss at ~350 K due to the evaporation of water molecules in the samples. After that, the sample shows a significant mass loss at ~548 K because the PSS components start to degrade<sup>[29]</sup>. When the temperature increases to 773 K, a further significant breakage of the PEDOT skeleton occurs, leading to another dramatic mass loss<sup>[30]</sup>. Thus, it is believed that PEDOT:PSS possesses excellent thermal stability under 470 K (the maximum testing temperature for TE and mechanical performances), below which the PEDOT:PSS will not experience any molecular degradation.

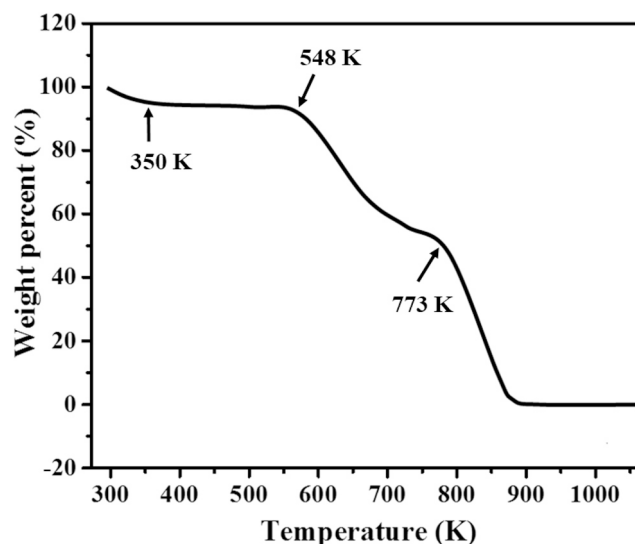


**Figure 3.** Thermogravimetric analysis curve of PEDOT:PSS-IL film. PEDOT:PSS: Poly(3,4-ethylenedioxythiophene):poly(styrene sulfonate); IL: ionic liquid.

Figure 4A displays the influence of temperature on the electrical conductivity for the composites with and without IL. It can be found that the electrical conductivity is dramatically enhanced at the same SWCNT content (30 or 60 wt.%) after the addition of IL additives. The IL additive interacts with PEDOT:PSS through an ion exchange effect, resulting in the transformation of the PEDOT conformation to a more conductive linear conformation and hence an improvement in the electrical conductivity<sup>[31-33]</sup>. Furthermore, the electrical conductivity decreases with increasing temperature from 293 to 470 K, exhibiting typical metal behavior<sup>[34]</sup>. In contrast, the Seebeck coefficients of the composites with and without IL increase distinctly with increasing temperature between 293 and 470 K [Figure 4B]. The addition of IL does not significantly affect the Seebeck coefficient if the experimental errors are considered. The variations of the electrical conductivity and the Seebeck coefficient are verified by the change in carrier concentration and mobility in Figure 4C and D. Compared to the IL-free composite (SWCNT content of 30 or 60 wt.%), both the carrier concentration and mobility are significantly improved for the composite with IL, which accounts for the dramatic increase in electrical conductivity after the addition of IL additives [Figure 4A]. In contrast, the Seebeck coefficient is negatively correlated with the carrier concentration and positively correlated with the carrier mobility<sup>[24,35]</sup>. The simultaneous carrier concentration and carrier mobility lead to a very slight variation in the Seebeck coefficient for the composites with and without IL [Figure 4B].

The *PF* values in Figure 4E show a positive temperature dependence for the composites with and without IL [Figure 4B]. The *PF* values of the composites with IL are always higher than the IL-free ones and the maximum *PF* value of 301.35  $\mu\text{W m}^{-1} \text{K}^{-2}$  is reached for PEDOT:PSS/SWCNT (60 wt.%) -IL composites at 470 K [Figure 4E]. The carrier transport mechanism is analyzed by the VRH model:

$$\sigma = \sigma_0 \exp \left[ - \left( \frac{T_0}{T} \right)^\alpha \right] \quad (2)$$

where  $\sigma_0$  represents the electrical conductivity at an infinite temperature (0 K),  $T_0$  is the characteristic temperature,  $T$  is the experimental temperature and the parameter  $\alpha$  is related to dimensionality via the expression of  $\alpha = 1/(1+D)$ <sup>[36,37]</sup>. The carrier transport mode can be judged by the  $\alpha$  values. Specifically, values of 1/2 and 1/4 correspond to one- and three-dimensional transport, respectively. The VRH model describes



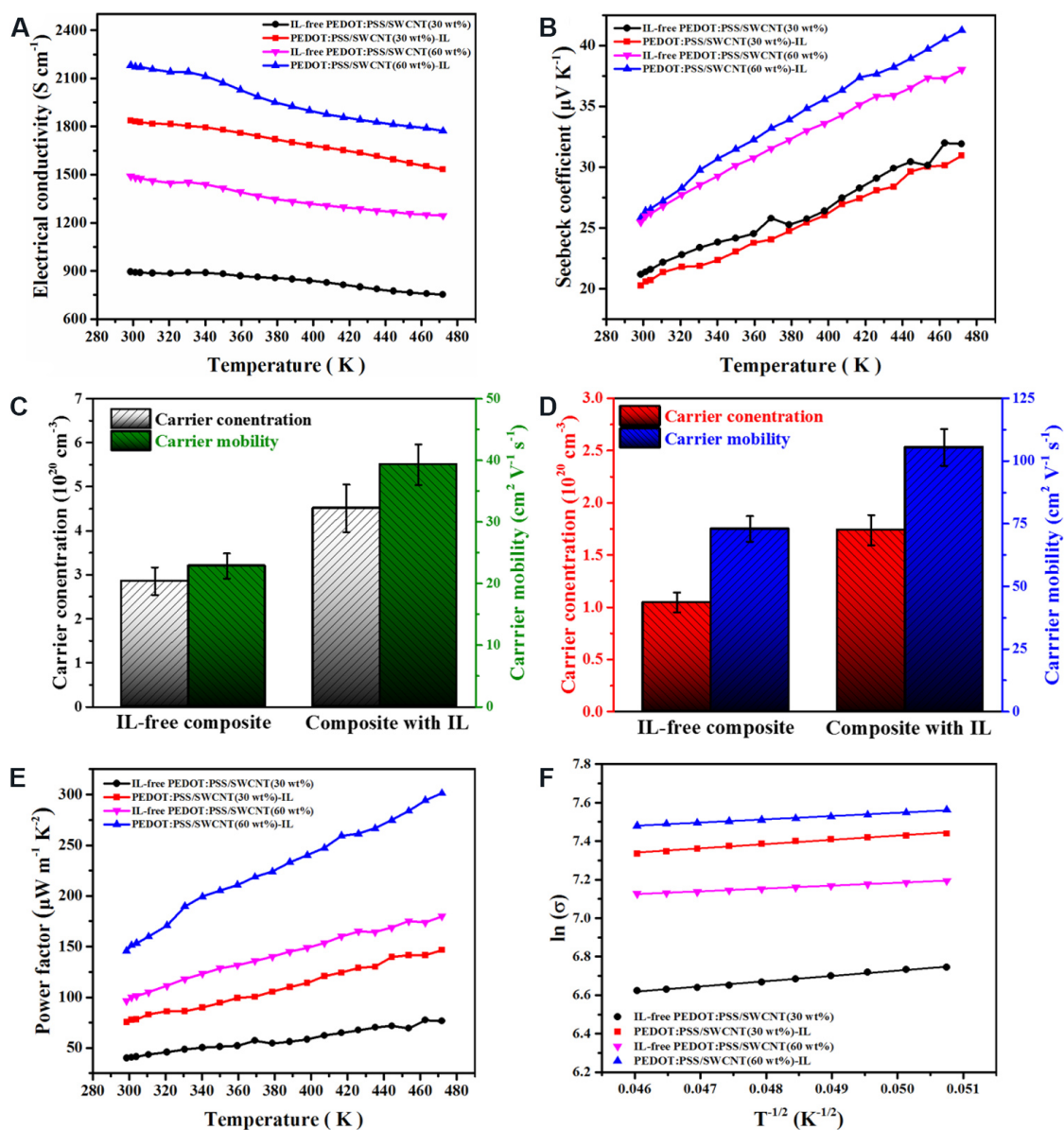


**Figure 4.** (A, B, E) TE parameters for the composites with and without IL containing SWCNT contents of 30 and 60 wt%. Comparison of carrier concentration and mobility of composites with and without IL at SWCNT contents of (C) 30 and (D) 60 wt%. (F) Dependence of  $\ln\sigma$  on  $T^{-1/2}$  for the composite with and without IL. TE: Thermoelectric; IL: ionic liquid; SWCNT: single-walled carbon nanotube.

the transport behavior of carriers in disordered systems in which the carrier hops from one localized site to another rather than the whole region<sup>[38,39]</sup>. In the present work,  $\ln\sigma$  shows an obvious linear relationship with  $T^{-1/2}$  for both composites at high temperatures in Figure 4F, suggesting that the carrier transport route of the PEDOT:PSS/SWCNT films is one-dimensional.

### Morphology and flexibility of composites with IL

Figure 5 compares the SEM images of the PEDOT:PSS/SWCNT-IL composites at room temperature and after the 470 K test. It can be seen that the SWCNT bundles are coated with PEDOT:PSS at room temperature [Figure 5A and C]. After the TE test at 470 K, some PEDOT:PSS components partially melted

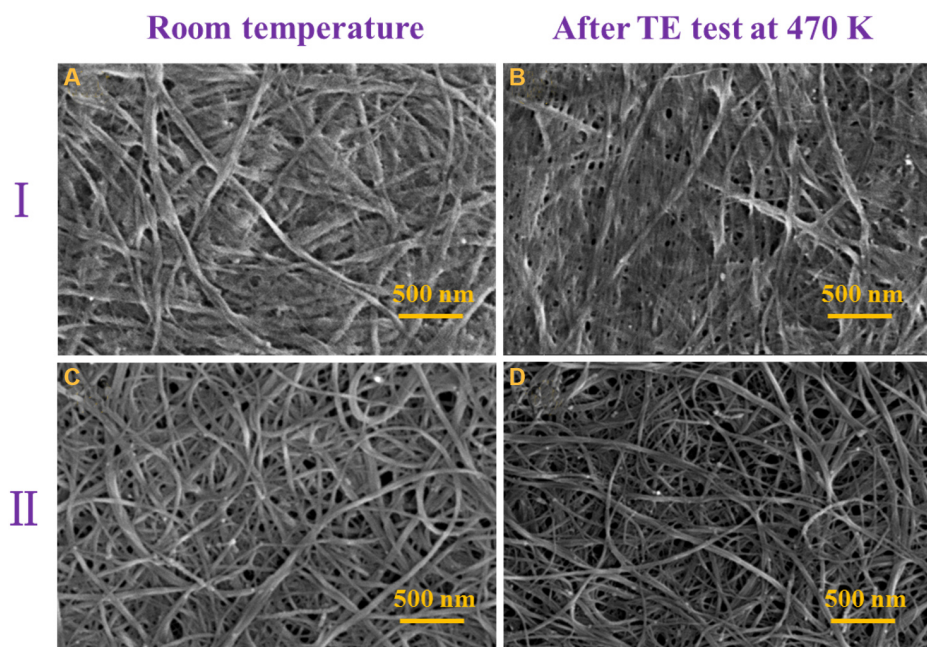


**Figure 5.** Typical scanning electronic microscopy images of PEDOT:PSS/SWCNT-IL composites with a SWCNT content of 30 (Row I) or 60 wt.% (Row II) after TE test at (A, C) room temperature and (B, D) after TE test at 470 K. PEDOT:PSS/SWCNT: Poly(3,4-ethylenedioxythiophene):poly(styrene sulfonate)/single-walled carbon nanotube; IL: ionic liquid.

and covered the surfaces of the SWCNT bundles, leading to a denser conductive network [Figure 5B and D]. Such a structure may be beneficial to the enhancement of the TE performance at high temperature.

Figure 6 presents optical photographs of the PEDOT:PSS/SWCNT-IL composite film (SWCNT content of 60%) at room temperature and after the high-temperature test. Evidently, the PEDOT:PSS/SWCNT-IL film can be easily bent and even wrapped around a rod with a radius of 1.5 mm without any obvious breakage [Figure 6A], indicating its high flexibility. This is consistent with our previous work<sup>[27]</sup>. After the high-temperature test (393 or 470 K), the PEDOT:PSS/SWCNT-IL composite still maintained its high flexibility [Figure 6B and C]. This characteristic is significant for the application of TE composites at high temperatures<sup>[40,41]</sup>.

### Mechanical properties of flexible composite films

Figure 7A-C shows the tensile-strain curves of the IL-free PEDOT:PSS/SWCNT and PEDOT:PSS/SWCNT-IL composites at room temperature, 393 K and 470 K. The samples at 393 and 470 K are represented by sample@393 K and sample@470 K, respectively. At room temperature [Figure 7A], the PEDOT:PSS/SWCNT-IL composite presents a steady enhancement in the elongation at break compared to IL-free PEDOT:PSS/SWCNT composite. Specifically, the elongation at break increases to 5.0% for the PEDOT:PSS/SWCNT-IL composites (30 wt.% SWCNTs) from 1.6% for the IL-free PEDOT:PSS/SWCNT composite (30 wt.% SWCNTs). A similar increase in the elongation at break is also obtained for the PEDOT:PSS/SWCNT-IL composites (60 wt.% SWCNTs). This is possibly due to the formation of a fibrillar PEDOT structure stemming from the modulation of the IL<sup>[42-44]</sup>. The role of the IL that can increase the elongation at break also can be demonstrated for the composites at 393 K [Figure 7B] and 470 K [Figure 7C]. Figure 7D compares the influence of temperature on the elongation at break of the composites with and without IL. These results suggest that increasing temperature can enhance the elongation at break

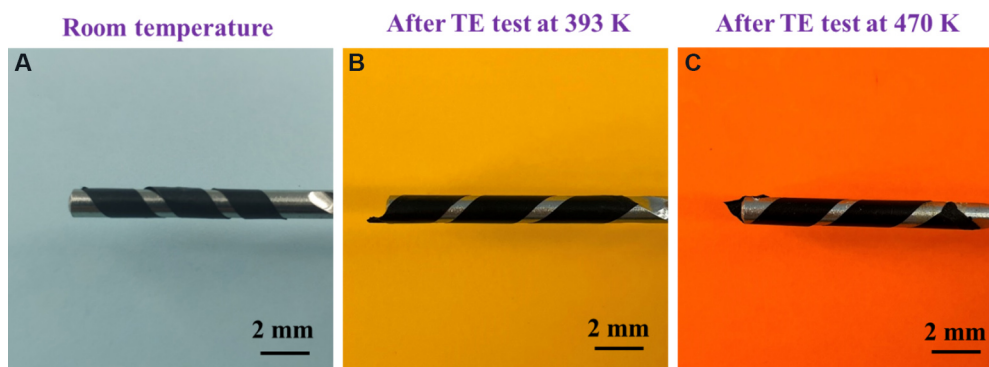


**Figure 6.** Optical photographs of PEDOT:PSS/SWCNT-IL composite film with 60 wt.% SWCNTs after TE test at (A) room temperature, (B) 393 K and (C) 470 K. PEDOT:PSS/SWCNT: Poly(3,4-ethylenedioxythiophene):poly(styrene sulfonate)/single-walled carbon nanotube; IL: ionic liquid; TE: thermoelectric.

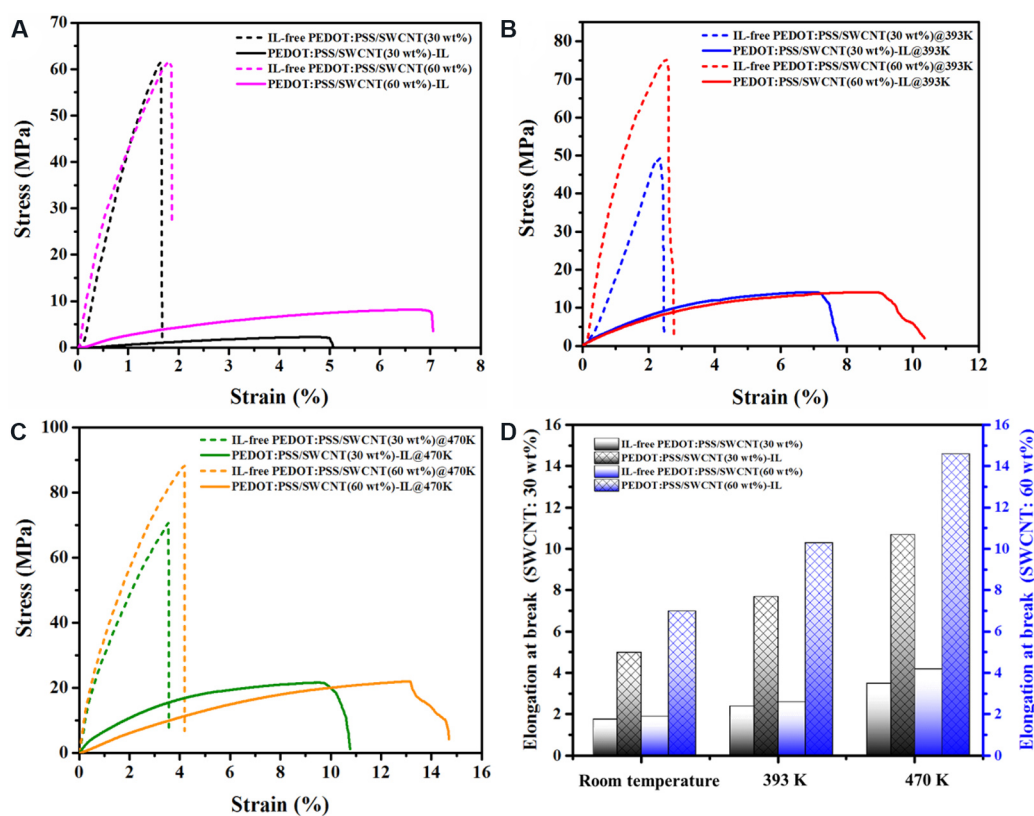


**Figure 7.** Stress-strain curves of PEDOT:PSS/SWCNT composite films with different SWCNT and IL contents at (A) room temperature, (B) 393 K and (C) 470 K. (D) Comparison of elongation at break of composites with and without IL. PEDOT:PSS/SWCNT: Poly(3,4-ethylenedioxythiophene):poly(styrene sulfonate)/single-walled carbon nanotube; IL: ionic liquid.

of the composites, which may result from the accelerating relaxation of polymer chains at high temperature<sup>[45]</sup>. Accordingly, the elongations at break can be improved by the addition of IL and the increasing temperature.



## CONCLUSIONS

In summary, we have reported the TE and mechanical properties of flexible IL-free PEDOT:PSS/SWCNT and PEDOT:PSS/SWCNT-IL composite films at different SWCNT contents and temperatures. The PEDOT:PSS/SWCNT-IL composites show higher TE performance than that of their IL-free counterparts with the same SWCNT contents at room and high temperatures. Both composites show increasing trends of *PF* values with increasing temperature. The maximum *PF* value of  $301.35 \mu\text{W m}^{-1} \text{K}^{-2}$  is obtained for the PEDOT:PSS/SWCNT-IL composite at 470 K. Furthermore, the addition of IL can improve the elongation at break of the composites compared to the IL-free composites. This work clarifies the influence of IL and temperature on the TE and mechanical properties of PEDOT:PSS-based composites and thus helps widen their applications at different temperature ranges.

## DECLARATIONS

### Authors' contributions

Experiments, data analysis, image editing, writing a draft: Deng W

Data discussion: Deng L

Data analysis: Hu Y

Reviewing and editing, supervision, funding acquisition: Zhang Y, Chen G

All authors have given approval to the final version of the manuscript.

### Availability of data and materials

Not applicable.

### Financial support and sponsorship

This work was financially supported by National Natural Science Foundation of China (No. 51973122), Guangdong Basic and Applied Basic Research Foundation (No. 2019A151511196) and the Opening Project of State Key Laboratory of Polymer Materials Engineering (Sichuan University) (Grant No. sklpme2021-05-06). We also acknowledge the SEM characterization provided by Instrumental Analysis Center of Shenzhen University (Lihu Campus).

### Conflicts of interest

All authors declared that there are no conflicts of interest.

### Ethical approval and consent to participate

Not applicable.

### Consent for publication

Not applicable.

### Copyright

© The Author(s) 2021.

## REFERENCES

1. Fan Z, Du D, Yao H, Ouyang J. Higher PEDOT molecular weight giving rise to higher thermoelectric property of PEDOT:PSS: a comparative study of clevis P and clevis PH1000. *ACS Appl Mater Interfaces* 2017;9:11732-8. DOI PubMed
2. Fan Z, Du D, Yu Z, Li P, Xia Y, Ouyang J. Significant enhancement in the thermoelectric properties of PEDOT:PSS films through a treatment with organic solutions of inorganic salts. *ACS Appl Mater Interfaces* 2016;8:23204-11. DOI PubMed
3. Li F, Cai K, Shen S, Chen S. Preparation and thermoelectric properties of reduced graphene oxide/PEDOT:PSS composite films. *Synth Met* 2014;197:58-61. DOI
4. Liang L, Fan J, Wang M, Chen G, Sun G. Ternary thermoelectric composites of polypyrrole/PEDOT:PSS/carbon nanotube with unique layered structure prepared by one-dimensional polymer nanostructure as template. *Compos Sci Technol* 2020;187:107948. DOI
5. Yin S, Lu W, Wu R, Fan W, Guo CY, Chen G. Poly(3,4-ethylenedioxythiophene)/Te/single-walled carbon nanotube composites with

- high thermoelectric performance promoted by electropolymerization. *ACS Appl Mater Interfaces* 2020;12:3547-53. DOI PubMed
6. Zhao J, Tan D, Chen G. A strategy to improve the thermoelectric performance of conducting polymer nanostructures. *J Mater Chem C* 2017;5:47-53. DOI
  7. Yu J, Zhang K, Deng Y. Recent progress in pressure and temperature tactile sensors: Principle, classification, integration and outlook. *Soft Sci* 2021;1:6. DOI
  8. Nath C, Kumar A, Kuo Y, Okram GS. High thermoelectric figure of merit in nanocrystalline polyaniline at low temperatures. *Appl Phys Lett* 2014;105:133108. DOI
  9. Zou Q, Shang H, Huang D, et al. Improved thermoelectric performance in n-type flexible Bi<sub>2</sub>Se<sub>3+x</sub>/PVDF composite films. *Soft Sci* 2021;1:2. DOI
  10. Xu B, Zhang J, Yu G, Ma S, Wang Y, Wang Y. Thermoelectric properties of monolayer Sb<sub>2</sub>Te<sub>3</sub>. *J Appl Phys* 2018;124:165104. DOI
  11. Das D, Malik K, Deb AK, Dhara S, Bandyopadhyay S, Banerjee A. Defect induced structural and thermoelectric properties of Sb<sub>2</sub>Te<sub>3</sub> alloy. *J Appl Phys* 2015;118:045102. DOI
  12. Kim N, Kee S, Lee SH, et al. Highly conductive PEDOT:PSS nanofibrils induced by solution-processed crystallization. *Adv Mater* 2014;26:2268-72, 2109. DOI PubMed
  13. Wang L, Zhang J, Guo Y, et al. Fabrication of core-shell structured poly(3,4-ethylenedioxythiophene)/carbon nanotube hybrids with enhanced thermoelectric power factors. *Carbon* 2019;148:290-6. DOI
  14. Fan W, Zhang Y, Guo C, Chen G. Toward high thermoelectric performance for polypyrrole composites by dynamic 3-phase interfacial electropolymerization and chemical doping of carbon nanotubes. *Compos Sci Technol* 2019;183:107794. DOI
  15. Wu J, Sun Y, Pei W, Huang L, Xu W, Zhang Q. Polypyrrole nanotube film for flexible thermoelectric application. *Synth Met* 2014;196:173-7. DOI
  16. Wu J, Sun Y, Xu W, Zhang Q. Investigating thermoelectric properties of doped polyaniline nanowires. *Synth Met* 2014;189:177-82. DOI
  17. Deng L, Huang X, Lv H, Zhang Y, Chen G. Unravelling the mechanism of processing protocols induced microstructure evolution on polymer thermoelectric performance. *Appl Mater Today* 2021;22:100959. DOI
  18. Qu D, Huang X, Li X, Wang H, Chen G. Annular flexible thermoelectric devices with integrated-module architecture. *npj Flex Electron* 2020;4. DOI
  19. Wang H, Yu C. Organic thermoelectrics: materials preparation, performance optimization, and device integration. *Joule* 2019;3:53-80. DOI
  20. Xia Y, Sun K, Ouyang J. Solution-processed metallic conducting polymer films as transparent electrode of optoelectronic devices. *Adv Mater* 2012;24:2436-40. DOI PubMed
  21. Zhang Y, Zheng D, Pang H, Tang J, Li Z. The effect of molecular chain polarity on electric field-induced aligned conductive carbon nanotube network formation in polymer melt. *Compos Sci Technol* 2012;72:1875-81. DOI
  22. Zhang Y, Zhang Q, Chen G. Carbon and carbon composites for thermoelectric applications. *Carbon Energy* 2020;2:408-36. DOI
  23. Wang X, Liang L, Lv H, Zhang Y, Chen G. Elastic aerogel thermoelectric generator with vertical temperature-difference architecture and compression-induced power enhancement. *Nano Energy* 2021;90:106577. DOI
  24. Li Z, Deng L, Lv H, et al. Mechanically robust and flexible films of ionic liquid-modulated polymer thermoelectric composites. *Adv Funct Mater* 2021;31:2104836. DOI
  25. Zhang Y, Deng L, Lv H, Chen G. Toward improved trade-off between thermoelectric and mechanical performances in polycarbonate/single-walled carbon nanotube composite films. *npj Flex Electron* 2020;4:26. DOI
  26. Taroni PJ, Santagiuliana G, Wan K, et al. Toward stretchable self-powered sensors based on the thermoelectric response of PEDOT:PSS/polyurethane blends. *Adv Funct Mater* 2018;28:1704285. DOI
  27. Deng W, Deng L, Li Z, Zhang Y, Chen G. Synergistically boosting thermoelectric performance of PEDOT:PSS/SWCNT composites via the ion-exchange effect and promoting SWCNT dispersion by the ionic liquid. *ACS Appl Mater Interfaces* 2021;13:12131-40. DOI PubMed
  28. Zhang Y, Fuentes CA, Koekoek R, et al. Spreading dynamics of molten polymer drops on glass substrates. *Langmuir* 2017;33:8447-54. DOI PubMed
  29. Friedel B, Keivanidis PE, Brenner TJK, et al. Effects of layer thickness and annealing of PEDOT:PSS layers in organic photodetectors. *Macromolecules* 2009;42:6741-7. DOI
  30. Gueye MN, Carella A, Massonnet N, et al. Structure and dopant engineering in PEDOT thin films: practical tools for a dramatic conductivity enhancement. *Chem Mater* 2016;28:3462-8. DOI
  31. Mazaheripour A, Majumdar S, Hanemann-rawlings D, et al. Tailoring the Seebeck coefficient of PEDOT:PSS by controlling ion stoichiometry in ionic liquid additives. *Chem Mater* 2018;30:4816-22. DOI
  32. Atoyo J, Burton MR, McGettrick J, Carnie MJ. Enhanced electrical conductivity and Seebeck coefficient in PEDOT:PSS via a two-step ionic liquid and NaBH<sub>4</sub> treatment for organic thermoelectrics. *Polymers (Basel)* 2020;12:559. DOI PubMed PMC
  33. Yemata TA, Zheng Y, Kyaw AKK, et al. Improved thermoelectric properties and environmental stability of conducting PEDOT:PSS films post-treated with imidazolium ionic liquids. *Front Chem* 2019;7:870. DOI PubMed PMC
  34. Fan W, Liang L, Zhang B, Guo C, Chen G. PEDOT thermoelectric composites with excellent power factors prepared by 3-phase interfacial electropolymerization and carbon nanotube chemical doping. *J Mater Chem A* 2019;7:13687-94. DOI
  35. Ziati M, Bekkioui N, Ez-zahraouy H. Correlation between carrier mobility and effective mass in Sr<sub>2</sub>RuO<sub>4-x</sub>F<sub>x</sub> (x = 2) under uniaxial strain using the Yukawa screened PBE0 hybrid functional. *J Phys Chem Solids* 2022;161:110409. DOI
  36. Huang X, Deng L, Liu F, Liu Z, Chen G. Aggregate structure evolution induced by annealing and subsequent solvent post-treatment

- for thermoelectric property enhancement of PEDOT:PSS films. *Chem Eng J* 2021;417:129230. DOI
37. Shante VKS, Varma CM, Bloch AN. Hopping conductivity in “one-dimensional” disordered compounds. *Phys Rev B* 1973;8:4885-9. DOI
38. Zhou X, Liang A, Pan C, Wang L. Effects of oxidative doping on the thermoelectric performance of polyfluorene derivatives/carbon nanotube composite films. *Org Electron* 2018;52:281-7. DOI
39. Wang S, Zhou Y, Liu Y, Wang L, Gao C. Enhanced thermoelectric properties of polyaniline/polypyrrole/carbon nanotube ternary composites by treatment with a secondary dopant using ferric chloride. *J Mater Chem C* 2020;8:528-35. DOI
40. Deng L, Zhang Y, Wei S, Lv H, Chen G. Highly foldable and flexible films of PEDOT:PSS/Xuan paper composites for thermoelectric applications. *J Mater Chem A* 2021;9:8317-24. DOI
41. Jia Y, Jiang Q, Sun H, et al. Wearable thermoelectric materials and devices for self-powered electronic systems. *Adv Mater* 2021;33:e2102990. DOI PubMed
42. Li Q, Zhou Q, Wen L, Liu W. Enhanced thermoelectric performances of flexible PEDOT:PSS film by synergistically tuning the ordering structure and oxidation state. *J Materiomics* 2020;6:119-27. DOI
43. Li Q, Deng M, Zhang S, et al. Synergistic enhancement of thermoelectric and mechanical performances of ionic liquid LiTFSI modulated PEDOT flexible films. *J Mater Chem C* 2019;7:4374-81. DOI
44. Kee S, Kim H, Paleti SHK, et al. Highly stretchable and air-stable PEDOT:PSS/ionic liquid composites for efficient organic thermoelectrics. *Chem Mater* 2019;31:3519-26. DOI
45. Zhang Y, Pang H, Dai K, et al. Conductive network formation during annealing of an oriented polyethylene-based composite. *J Mater Sci* 2012;47:3713-9. DOI